(1972).
[38]J. G. Hirschberg and P. Platz, Appl. Opt. 4, 1375 (1965).
[39]M. Daehler, G. A. Sawyer, and K. S. Thomas, Phys. Fluids 12, 225 (1969).
[40]E. Glock, *Proceedings of the Seventh International Conference on Ionization Phenomena in Gases, Belgrade*, 1965 (Gradjevinska Knjiga Publishing House, Belgrade, Yugoslavia, 1965), Vol. 3, p. 194.
[41]A. D. Beach. J. Sci. Instr. 44, 690 (1967).
[42]C. Longmire, J. L. Tuck, and W. B. Thompson, *Plasma Physics and Themonuclear Research* (MacMillan, New York, 1965), Vol. 1, pp. 216–222.
[43]Lord Rayleigh, Phil. Mag. 47, 379 (1899).
[44]S. Glasstone and R. H. Loveberg, *Controlled Thermonuclear Reactions* (Van Nostrand, New York, 1960), p. 20.

PHYSICAL REVIEW A VOLUME 6, NUMBER 2 AUGUST 1972

Experimental Indications of Plasma Instabilities Induced by Laser Heating*

J. W. Shearer, S. W. Mead, J. Petruzzi, F. Rainer, J. E. Swain, and C. E. Violet
Lawrence Livermore Laboratory, University of California, Livermore, California 94550
(Received 20 December 1971)

The detection of ~ 100-keV x radiation and of directly back-scattered light is described for neodymium-glass-laser light pulses focused on a polyethylene target. These observations can be explained in terms of the nonlinear excitation of plasma waves by the laser light.

We recently made some measurements of x rays and light reflection from a laser-produced plasma which suggest that plasma instabilities have been produced. Our neodymium laser, which includes a multipass glass-disk system, has been described elsewhere.[1–3] The 1.06-μm-wavelength neodymium-laser light was focused by means of an $f/7$ lens to an irregular-shaped spot with a mean diameter of approximately 80 μm.[3] The pulse energy ranged from 20 to 70 J; the pulse length ranged from 2 to 5 nsec. The maximum power during the pulse was 10 GW, corresponding to an intensity at the target of $\simeq 2\times 10^{14}$ W/cm^2.

The laser pulse was focused on flat targets of "deuterated" and ordinary polyethylene, $(CD_2)_n$ and $(CH_2)_n$, respectively. The targets were tilted about 5° to prevent back reflections from causing spontaneous oscillations in the laser amplifier chain. After each shot the target was moved to expose a fresh new surface. It was found necessary to wait 1 h between shots to allow the disk laser to cool. Failure to allow ample cooling resulted in a larger focal spot and a decrease or an absence of neutrons and hard x rays.

Diagnostics for the first set of experiments included a large plastic scintillation counter, intended for neutron detection and located in close proximity to the laser target. The detector was initially shielded with 9.5 mm of aluminum plus 6.3 mm of lead. Nevertheless, when the laser was fired, scintillation pulses were seen from the $(CH_2)_n$ target as well as from $(CD_2)_n$. When the shielding thickness was increased to 9.5 mm of aluminum plus 12.7 mm of lead, no pulses were seen when the $(CH_2)_n$ target was in place, but small pulses corresponding to 10^3 and 10^4 neutrons were seen when the $(CD_2)_n$ target was used.[3–5]

The fact that large pulses were seen from a $(CH_2)_n$ target with a scintillation detector shielded by 6.3 mm of lead was interpreted as evidence that considerable quantities of hard x rays were being produced in these experiments. Similar hard x radiation has been reported recently by the Lebedev group in the USSR.[6]

To measure the x-ray spectrum more accurately, additional measurements were taken with four scintillation detectors using a target of polyvinyl chloride. One pair of detectors used europium-activated calcium fluoride fluors in conjunction with aluminum absorbers; the other pair used thallium-activated sodium iodide fluors and nickel absorbers. To minimize background corrections, the nickel-absorber pair was shielded from scattered hard x rays by at least 6 mm of lead on all sides, except for a narrow cone pointed at the focal spot. The aluminum-absorber pair did not need such shielding, because the soft-x-ray signal was much greater than the hard-x-ray background. The absorption ratios for a given absorber pair were normalized by means of supplementary measurements made with equal absorber thicknesses. An apparent electron temperature T was computed from the measured absorption ratio using the curves computed by Elton.[7]

Some representative results of these measurements are presented in Table I; they indicate that the transmission ratio for the nickel pair corresponds to a much higher temperature than the corresponding ratio for the aluminum pair. In addition to the results given in the table, we made a

TABLE I. X-ray absorption ratios for four C_2H_3Cl target experiments.

Shot number	Laser pulse[a] (J)	Aluminum R[b]	Aluminum E[c] (keV)	Aluminum T[d] (keV)	Nickel R[e]	Nickel E[c] (keV)	Nickel T[d] (keV)
1	43	2.8	8.0	1.7	3.8	116	48
2	45	2.5	8.3	2.0	4.4	112	41
3	49	2.3	8.5	2.3	4.8	108	37
4	42	2.4	8.4	2.2	3.5	120	53

[a]Half-width 5 nsec. See profile in Fig. 2(a).

[b]Ratio of integrated signal outputs for aluminum absorbers of 0.0206 and 0.0412 g/cm^2.

[c]An "average" energy E for the x rays computed by assuming exponential absorption of a monoenergetic spectrum.

[d]The estimate for bremsstrahlung temperature T computed from the curves in Ref. 7.

[e]Ratio of integrated signal outputs for nickel absorbers of 1.40 and 5.60 g/cm^2.

number of measurements with thinner aluminum foils (0.007 and 0.014 g/cm^2). The ratios observed in these measurements correspond to electron temperatures of about 0.5 keV and are in agreement with previous measurements of other workers.[8] Numerical hydrodynamic computations[9,10] of the laser-heated plasma produced by this focused intensity have indicated maximum electron temperatures of the order of 1.0 keV.

Since our measurements were integrated over the target in both time and space, we sampled a distribution of temperatures. Furthermore, the x rays penetrating the thick absorbers are selectively representative of the higher-temperature material. Therefore, the thicker-aluminum-absorber measurements in Table I might be interpreted as being representative of the temperature of some particularly hot spot of the target, although this is a somewhat higher temperature than expected.

On the other hand, the measurements reported here for the nickel-absorber ratio do not agree at all with our expectations for the electron temperature. The values of 37 to 53 keV are not compatible in any way with our predictions for the maximum electron temperature; they are an order of magnitude too high. The results suggest that a unique electron temperature does not exist and that an anomalous heating of some of the electrons has taken place.

The disparity between our experimental results and the results expected for a plasma with a temperature of about 1 keV can be emphasized by a comparison of absorption curves. A single absorption curve involving data obtained with dissimilar absorbing materials can be approximated to the extent that absorption in the energy region of principal importance is a result of the photoelectric effect and does not involve significant absorption-edge discontinuities. In such a region, the mass absorption coefficient μ can be represented to a good approximation in the form

$$\ln R/X \equiv \mu \cong M/k^m , \tag{1}$$

where R is the intensity ratio for the absorber thickness X for a monoenergetic x-ray beam of quantum energy $k = h\nu$, and M and m are constants. In the energy regime where photoelectric effect is dominant, $m = 3$. For the aluminum absorbers used here, $M = 2.7 \times 10^4$ keV^3 cm^2 g^{-1}; for nickel, $M = 2.6 \times 10^5$ in the same units. Thus we can, in an approximate manner, express the aluminum and nickel results in terms of a common thickness parameter MX as is done for one of our experiments in Fig. 1. Similar curves were obtained for our other data.

The ordinate E_0 in Fig. 1 is estimated from the solid angle of the detector, its light efficiencies, gain, and other electrical constants. Not all of these parameters are as well known as we would wish, but we believe that our estimate of E_0 is accurate enough for a rough comparison between the aluminum- and nickel-absorber results. In Fig. 1 we have also fitted the bremsstrahlung absorption curves for temperatures of 2 and 40 keV (calculated from Ref. 7) to the aluminum and nickel ratios, respectively. The excess of high-energy x rays implied by our experimental data is clearly evident.

Recently, x-ray spectra from plasma-focus experiments have been reported in terms of a power law,[11,12]

$$\frac{dI}{dk} \equiv \frac{A}{k^l} , \tag{2}$$

where A and the power l are constants. Because the plasma focus and the laser-produced plasma have similar densities ($\simeq 10^{20} - 10^{22}$ cm^{-3}), it is of interest to compare these spectra. To do this, we must unfold our absorption data to obtain the exponent l. We note that E_0, the ordinate of Fig. 1, can be written

$$E_0 = 4\pi r^2 \int_0^\infty \frac{dI}{dk} e^{-\mu X} dk , \tag{3}$$

where r is the radius at which the intensity constant A is evaluated. Substituting Eqs. (1) and (2) and integrating, one obtains

$$E_0 = (4\pi r^2 A) \frac{\Gamma(n)}{mM^n} \frac{1}{X^n} , \tag{4}$$

where the exponent n is given by

$$n = (l-1)/m . \tag{5}$$

Rearrangement of these equations enables us to solve for the exponent l in terms of experimental

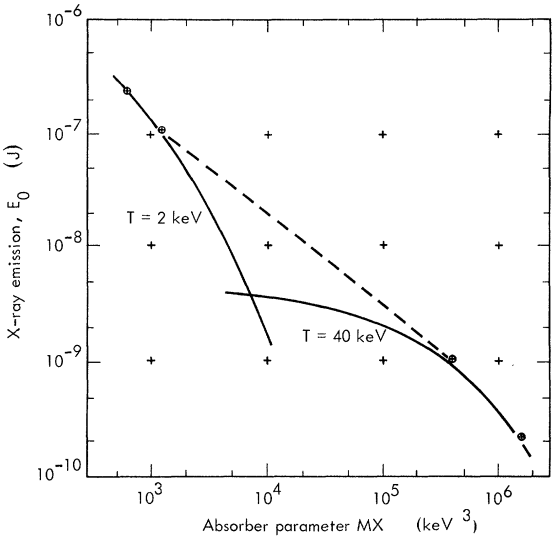

FIG. 1. X-ray absorption curve for shot 3, based on the four measured points as described in the text. The two temperature curves were calculated from Ref. 7.

quantities:

$$l = 1 + m \frac{\ln(E_1/E_2)}{\ln(M_2X_2/M_1X_1)} , \qquad (6)$$

where the subscripts 1 and 2 refer to two different absorption measurements. For the data presented in Fig. 1, we obtain an exponent of 4.7 from the aluminum-pair ratio and an exponent of 3.4 from the aluminum-to-nickel ratio. These are approximately the same as the plasma-focus exponents reported previously.[11,12] The nickel-pair ratio for hard x rays was not evaluated by this technique because the Compton effect distorts the value of m in that spectral region.

In addition to neutron and x-ray measurements, the reflection of the 1.06-μm neodymium-laser light was monitored with calibrated photodiode detectors and compared with the incident light. Figure 2 is a plot of five such measurements, including shot 3 of Fig. 1. The latter also includes a light-transmission measurement made through the polyvinyl chloride target. It is seen that the reflected pulse has a different shape than the incident-light pulse; in particular, sharp bursts of reflected light are seen, beginning 2 to 5 nsec after the onset of the incident pulse.

These results are different from previous reflected-light measurements obtained by the group at Limeil,[13] but we believe that there are significant differences in the experimental conditions. The Limeil group used an $f/1$ focusing lens (which corresponds to a solid angle of 0.66 sr), and they measured a reflection coefficient of 30 to 40%. We used an $f/7$ focusing lens whose solid angle is 0.016 sr.

We recall that for focal-spot sizes of $\simeq 100$-μm diameter or less and laser-light pulses of $\simeq 1$ nsec or more, the plasma plume will expand sideways as well as toward the laser light.[5] The reason for this, of course, is that the rarefaction waves will move into the plume at velocities greater than $\simeq 10^7$ cm/sec. In this case, most of the laser light will encounter the plasma density gradient at oblique incidence[14]; therefore, the angle between most of the reflected light and the incident light will be greater than the 4° angle subtended by our lens. Consequently, it is not surprising that we see much less reflected light than the $f/1$ lens measurements of 30 to 40%. If we multiply the $f/1$ lens measurements by the ratio of the solid angles of the two lenses, we obtain a result of about 0.8% reflection, which is in agreement with our measurements of 0.5 to 1.0% (Fig. 2).

The bursts of reflected radiation that we observe have not been reported elsewhere, to our knowledge. In some cases, such as Figs. 2(d) and 2(e), they amount to more than 2 to 3% of the incident power. This intensity cannot be isotropic because it would then exceed 100% of the incident light. If the bursts fill only a small solid angle, they would probably not be easily seen through an $f/1$ lens. From these considerations, we conclude that the reflected-light bursts are preferentially emitted in the backward direction with respect to the incident light. In that case, a plausible explanation is that a backward-stimulated light beam is tracing out the same optical path as the incident light. In this situation it will be aimed back toward the focusing lens even in the presence of oblique density gradients that scatter the ordinary reflected light into larger angles.

The delay in the onset of these light-reflection bursts is believed to be due to the finite time required to build up a sufficiently thick plasma in which such nonlinear optics effects can grow.[15] The light-penetration curve measured in Fig. 2(a) is in qualitative agreement with this assumption, since it falls rapidly as the pulse develops. Presumably, at late times only the fringes of the focal spot can penetrate the target, because there the plasma has not yet been developed.

Another characteristic of these experiments is that there are positive shot-to-shot correlations between the occurrence of the light-reflection burst, the neutron pulses [from $(CD_2)_n$], and the hard-x-ray intensity. These correlations are, at present, only a qualitative observation made under a variety of experimental conditions.[3] However, similar correlations among reflected-light energy, x-ray emission, fast-ion emission, and neutrons have been reported elsewhere.[16,17]

In view of all our results, it is tempting to explain these observations by one basic phenomenon,

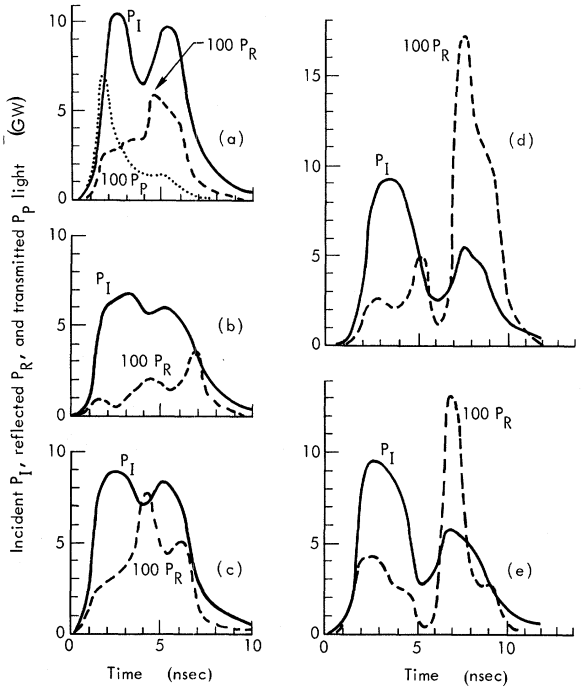

FIG. 2. Incident P_I, reflected P_R, and transmitted P_P light curves vs time for five different experiments on polyvinyl targets C_2H_3Cl. Figure 2(a) is shot 3, the same one as in Fig. 1. The other curves are for various earlier experiments, for which transmitted-light measurements were not taken. The normalization in time is estimated to be accurate within 1 nsec.

plasma instabilities. The x-ray results seem to be best explained by the parametric ion-acoustic instability[18-20] in which an incident electromagnetic wave of frequency ω_0 is coupled to an electron plasma wave of frequency $\simeq \omega_{pe}$ and to an ion-acoustic wave of frequency $\omega_a \simeq \omega_0 - \omega_{pe}$. The two plasma waves grow at the expense of the laser wave, reaching a large intensity that distorts the electron-velocity distribution function. A few high-energy electrons are accelerated thus creating the observed high-energy x rays by means of the bremsstrahlung process.

The threshold intensity I_T for the parametric instability can be written

$$I_T = 4cn N_e kT_e \left(\frac{\nu_a}{\omega_a}\right)\left(\frac{\nu_e}{\omega_{pe}}\right), \qquad (7)$$

where n is the plasma index of refraction, N_e is the electron density, and ν_a, ν_e are the damping rates for the acoustic and plasma waves, respectively. The lowest value of this threshold intensity is found at a plasma density N_e close to the cutoff density N_c, because at smaller densities the Landau damping is very large for the electrons. Thus, if we choose $N_e \simeq 0.9N_c$, then only collisional damping will be important for the electron wave. At this density, the refractive index $n \simeq 0.3$. Next, we use the laser-plume computer calculations[9,10] to estimate typical plasma temperatures of $T_e \simeq 0.5$ keV $\simeq T_i$ from which we can find that the acoustic-wave damping ratio ν_a/ω_a is about unity and the plasma-wave damping ratio is about 0.001.

Substituting back into Eq. (7), we arrive at an estimate for the threshold intensity of about 6×10^{12} W/cm^2. This threshold may be as much as one or two orders of magnitude higher in steep density gradients[15] where the plasma waves and acoustic waves transport energy from the region of lowest threshold. However, our average intensity is a factor of 30 higher than the minimum threshold estimate. Furthermore, we have recently examined our laser pulse with improved time resolution and have found preliminary evidence that the incident laser pulse contains many subnanosecond "spikes," which would imply intensities greater than 10^{15} W/cm^2 at the target. We therefore conclude that our highest incident intensities exceed the threshold for the excitation of the parametric ion-acoustic instability.

Next, we consider how a suprathermal-high-velocity-electron spectrum can be created by the unstable plasma. First, we note that the coherent "quivering" velocity of the electron in the high-frequency electromagnetic field is not great enough at these intensities to account for the observed high-energy x rays. An elementary calculation gives average quivering energies of 0.03 to 0.3 keV at intensities of 10^{14} to 10^{15} W/cm^2 when the plasma density is $N_e = 0.9N_c$. However, the plasma oscillations induced by the instability provide a mechanism for electron acceleration. This is most clearly shown in plasma-simulation computations,[21,22] where a significant high-energy "tail" is observed to appear in the electron-velocity distribution function after saturation of the linear-growth phase of the instability. The tail consists of electrons that are pulled out of the thermal distribution and accelerated to the phase velocity of some of the plasma waves. A significant enhancement in the number of electrons at higher velocities is observed. The effect is apparent for electrons having velocities up to ten times the thermal velocity, where the statistics of the available number of particles in the computation becomes too small for accuracy. This corresponds to a hundredfold increase in the energy of such electrons above the average thermal energy. This increase is sufficient to explain the 40-keV apparent temperature obtained in our x-ray experiments.

We conclude from these considerations that the parametric ion-acoustic instability is capable of explaining our experimental results. Another related instability, the so-called "growing mode" or

"oscillating two-stream instability,"[19,20] may also contribute to the absorption. We have not considered it in detail because its threshold is usually calculated to be somewhat higher than the parametric threshold and because it occurs at the cutoff density, further inside the plasma than the region where the parametric instability occurs.

The pulses of backward-directed light seem to be best explained by simulated Brillouin scattering[23,24] in which the incident electromagnetic wave of frequency ω_0 is reflected backward from an acoustic wave of frequency ω_a at a Stokes frequency of $\omega_0 - \omega_a$. The threshold intensity is also given by Eq. (7), where the damping constant ν_e is reinterpreted to mean only the collisional damping constant ν_{ei} and does not include Landau damping. Thus, this effect can occur at all plasma densities, although the growth rates are smaller than for the parametric instability.

Furthermore, the Brillouin instability need not grow up from the plasma noise level in our particular experiments. The reason is that the unabsorbed incident radiation is reflected when it reaches the vicinity of the cutoff density, so that a backward-light flux always exists. If the frequency width of the incident laser light is greater than the Stokes shift ω_a, then it is more likely that the observed reflected-light pulses are stimulated by the backward flux than that a Stokes wave will grow from the noise level. To estimate the frequency shift, we use the approximate momentum-conservation relation for backward Brillouin scattering:

$$2K_L \cong K_a , \tag{8}$$

from which one can obtain the frequency ratio:

$$\omega_a/\omega_0 \cong 2nv_a/c , \tag{9}$$

where v_a is the acoustic velocity. Using the same plasma conditions as before ($n = 0.3$, $T_e = T_i = 0.5$ keV), we obtain a wavelength shift of about 5 Å for a neodymium-laser beam. This is well within the recently observed spectrum width of our laser beam, where most of the energy is found within a wavelength band of 20 to 50 Å (varying from pulse to pulse). In this connection we have not yet measured the spectrum of the reflected light. The interpretation of such spectra is complicated by Doppler shifts and line structure, and we have not been able to decide on a clear relationship between our results and spectrum measurements obtained by other investigators.[25,26]

Evidence for similar plasma instabilities and anomalous absorption has been reported for ionospheric-heating experiments with 50-m radio waves[27] and in plasma experiments with microwaves.[28] Our results extend the range of observations to laser-light wavelengths. The effect of instabilities on the neutron emission is discussed elsewhere.[5]

The authors would like to acknowledge numerous discussions with R. E. Kidder and S. Bodner as well as assistance with the experiments by R. Dunham, B. Jackson, and R. Poli.

---

*This work was performed under the auspices of the U. S. Atomic Energy Commission and sponsored in part by the Defense Nuclear Agency.

[1]J. E. Swain, R. E. Kidder, K. Pettipiece, F. Rainer, E. D. Baird, and B. Loth, J. Appl. Phys. 40, 3973 (1969).

[2]G. B. Lubkin, Phys. Today 22, No. 11, 55 (1969). (1969).

[3]S. W. Mead, R. E. Kidder, J. E. Swain, F. Rainer, and J. Petruzzi, App. Opt. 11, 345 (1972).

[4]F. Floux, D. Cognard, L. G. Denoeud, G. Piar, D. Parisot, J. L. Bobin, F. Delobeau, and C. Fauquignon, Phys. Rev. A 1, 821 (1970).

[5]S. Bodner, G. Chapline, and J. S. DeGroot, Lawrence Livermore Laboratory Report No. UCRL-73425, 1971 (unpublished).

[6]N. G. Basov, V. A. Boiko, S. M. Zakharov, O. N. Krokhin, and G. V. Sklizkov, Zh. Eksperim. i Teor. Fiz. Pis'ma v Redaktsiyu 13, 691 (1971) [Sov. Phys. JETP Letters 13, 489 (1971)].

[7]R. C. Elton, Naval Research Laboratory, Washington, D. C., NRL Report No. 6738, 1968 (unpublished).

[8]J. L. Bobin, F. Delobeau, G. DeGiovanni, C. Fauquignon, and F. Floux, Nucl. Fusion 9, 115 (1969).

[9]R. E. Kidder, "Interaction of Intense Photon and Electron Beams with Plasmas," in *Physics of High Energy Density*, edited by P. Caldirola and H. Knoepfel (Academic, New York, 1971), pp. 306–352.

[10]J. W. Shearer and W. S. Barnes, "Numerical Calculations of Plasma Heating by Means of Subnanosecond Laser Pulses," in *Laser Interaction and Related Plasma Phenomena*, edited by H. J. Schwarz and H. Hora (Plenum, New York, 1971), pp. 307–337.

[11]H. L. L. van Paassen, R. H. Vandre, and R. Stephen White, Phys. Fluids 13, 2606 (1970).

[12]J. H. Lee, D. S. Loebbaka, and C. E. Roos, Plasma Phys. 13, 347 (1971).

[13]F. Floux, J. F. Benard, D. Cognard, and A. Saleres (unpublished).

[14]J. W. Shearer, Phys. Fluids 14, 183 (1971).

[15]F. W. Perkins and J. Flick, Phys. Fluids 14, 2012 (1971).

[16]K. Büchl, K. Eidmann, P. Mulser, H. Salzmann, and R. Sigel, Max-Planck-Institut für Plasmaphysik, Report No. IPP IV/28, 1971 (unpublished).

[17]C. Yamanaka, T. Yamanaka, T. Sasaki, K. Yoshida, M. Waki, and H. Kang, Institute of Plasma Physics, Nagoya University, Report No. IPPJ-117, 1972 (unpublished).

[18]D. F. DuBois and M. V. Goldman, Phys. Rev. Letters 14, 544 (1965).

[19]K. Nishikawa, J. Phys. Soc. Japan 24, 1152 (1968).

[20]P. K. Kaw and J. M. Dawson, Phys. Fluids 12, 2586 (1969).

[21]W. L. Kreuer and J. M. Dawson, Phys. Rev. Letters 25, 1174 (1970).
[22]J. DeGroot (private communication).
[23]A. J. Palmer, Phys. Fluids 14, 2714 (1971).
[24]S. E. Bodner and J. L. Eddleman, Lawrence Livermore Laboratory Report No. UCRL-73378, 1971 (unpublished).
[25]P. Belland, C. DeMichelis, M. Mattioli, and R. Papoular, Appl. Phys. Letters 18, 542 (1971).
[26]K. Büchl, K. Eidmann, H. Salzmann, and R. Sigel, Appl. Phys. Letters 20, 3 (1972).
[27]F. W. Perkins and P. K. Kaw, J. Geophys. Res. 76, 282 (1971).
[28]H. Dreicer, D. B. Henderson, and J. C. Ingraham, Phys. Rev. Letters 26, 1616 (1971).

PHYSICAL REVIEW A VOLUME 6, NUMBER 2 AUGUST 1972

Theory of Electrical Resistivity

V. M. Kenkre*‡ and M. Dresden†
Institute for Theoretical Physics, State University of New York, Stony Brook, New York 11790
(Received 13 March 1972)

A new general expression for the electrical resistivity of a substance is obtained with the help of projection techniques with the Liouville equation as the point of departure. No many-body detail is sacrificed and the "$\lambda^2 t$ limit" is not invoked. The first-order result in a perturbation expansion in orders of the scattering is presented in explicit form and shown to have a simple and physical appearance. It is also shown to reduce to the well-known Boltzmann expressions for simple cases.

I. INTRODUCTION

The calculation of the electrical resistivity of a substance can be performed at three different levels. The most elementary is the Drude approach,[1] wherein the electrons are assumed to be subjected to a viscous force proportional to their speed. Writing the classical Newtonian equation for each electron as

$$m\,\frac{d\vec{v}}{dt} = e\vec{E} - \alpha\vec{v}\,, \tag{1}$$

where the electron has mass m, charge e, and velocity $\vec{v}$, $\vec{E}$ is the applied electric field, and α is a constant of proportionality, we can immediately calculate the steady-state ($d\vec{v}/dt = 0$) electrical resistivity γ as

$$\gamma = m/Ne^2\tau\,, \tag{2a}$$

$$\tau = m/\alpha\,, \tag{2b}$$

where N is the total number of electrons in the substance and τ is the "relaxation time."

Apart from the fact that the equation of motion used is a classical one, the major drawback of the Drude approach is that its implicit assumption of a constant α (and therefore of a constant τ) cannot be justified and an investigation of the origin of the viscous force cannot be carried out within its framework. One merely makes general statements asserting that the viscous force arises from collisions of the electron with the scattering centers (other electrons or different bodies) and that the "relaxation time τ" is approximately one-half the average time between two collisions.

A more sophisticated approach starts with the Boltzmann equation,[2-7] which describes the time evolution of f, the ensemble density in μ space. The equation in its exact form is a complicated nonlinear integrodifferential one, and so approximations like "linearization" and the "relaxation-time assumption" (see for instance Ref. 3) are often used to solve for f.[8] From f one then obtains the electrical conductivity σ (which is of course $1/\gamma$) as[7]

$$\sigma = -\frac{e^2}{4\pi^3}\int \tau_k v_k^2\,\frac{\partial f_k^0}{\partial \epsilon_k}\,d^3k\,, \tag{3}$$

where v_k is the component of the velocity of the electron in state k along the direction of measurement, ϵ_k is its energy, f_k^0 is the equilibrium Fermi-Dirac distribution function, d^3k is a volume element in k space, and τ_k is the relaxation time which arises out of the relaxation-time assumption.

The above approach is widely used for practical calculations and almost all discussions of electrical resistivity or related problems are carried out in its context. Under these circumstances it is easy to forget its inherent limitations and the criticisms that can be levied against it. The most serious objection to this Boltzmann approach consists of an objection to the very use of the Boltzmann equation. This equation was derived[9] on the basis of intuitive arguments which are not rigorous and attempts to obtain it deductively from more general starting points (like for